

Electronic control of magnonic and spintronic devices

C. Tannous

*Laboratoire de Magnétisme de Bretagne, UBO CNRS-FRE 3117,
6 Avenue le Gorgeu C.S.93837, 29238 Brest Cedex 3, FRANCE.*

J. Gieraltowski

*Laboratoire des Domaines Océaniques, IUEM CNRS-UMR 6538,
Technopôle Brest Iroise, 29280 Plouzané, FRANCE.*

Nanometric magnonic and spintronic devices need magnetic field control in addition to conventional electronic control. In this work we review ways to replace magnetic field control by an electronic one in order to circumvent appearance of stray magnetic fields or the difficulty of creating large magnetic fields over nanometric distances. Voltage control is compared to current control and corresponding devices are compared from their energetic efficiency point of view.

PACS numbers: 85.75.-d, 85.75.-d, 75.76.+j, 75.30.Ds

Keywords: Magnetoelectronics, Spintronics, Spin transport effects, Spin waves

Version: April 20, 2022

1. INTRODUCTION

Minimal feature in microelectronics CMOS planar technology progressed from 22 nm in 2012 to its present value of 14 nm and is slated to reach 10 nm in 2016.

Progressing toward nanoelectronics with a minimal feature approaching steadily the nanometer limit leads to at least five major consequences:

1. Joule effect increase.

2. Interconnection delay increase.

3. Circuit size decrease with respect to some reference electromagnetic (EM) wavelength.

4. Enhancement of quantum effects.

5. Emergence of spin degrees of freedom.

Joule effect enhancement is due to resistor R scaling by a factor $s > 1$ increasing the resistance to sR whereas wire (interconnection) delay increase is due to rise of communicating wire length with number of components (see Table 1).

Microprocessor (year)	Feature Size (nm)	Transistors	Frequency (MHz)	Pins	Power consumption (Watts)	Wire Delay (clock cycle/cm)
Intel 4004 (1971)	10,000	2,300	0.750	16	1	1/1,000
Pentium IV-670 (2005)	90	169 million	3,800	775	115	4
(2005)/(1971) Ratio	(1/111)	73,478	5,066	48	115	4,000

TABLE 1: Comparison of two CPU characteristics dating from 1971 and 2005 and the evolution of their intrinsic properties with feature size decrease. The 4004 is the first commercial 4-bit CPU whereas the Pentium IV-670 is a single-core 64-bit CPU. As number of transistors, frequency, number of pins all increase as expected, wire delay and power consumption increase against all expectations. Wire delay is extracted from the speed of an electronic signal which is about 20 cm per nanosecond (ns) within the wire. Hence one gets 0.5 ns for a 10 cm propagation length and in the case of a 1 GHz CPU, the delay represents half-a-clock cycle.

While Joule effect and interconnection delay have been somehow virtually solved in microprocessors by introducing multi-core architecture (see Table 1), the latter concept appears as an intermediate solution awaiting a better technology to address, in a deeper way, power consumption and wire delays in devices.

Power consumption issue is tackled in magnonic and

spintronic devices that are based respectively on spin-wave and spin current manipulation. Extremely low power dissipation is reached in both cases (except with spin-transfer torque (STT) currents where critical density required for switching is very large as described in next section) since no Joule effect is expected when no charges are moving in order to carry information. Un-

dulation of spin moments is the carrier of information transport.

Magnonics belong to a class of devices based on spin waves to carry and process information on the nanoscale.

They are the magnetic counterpart of plasmons that are used in nanophotonics since the wavelength λ of magnons is orders of magnitude shorter than that of EM waves (photons) of the same frequency. Thus magnonic devices represent a serious step toward the fabrication of nanometer-scale microwave devices.

In nanophotonics surface plasmons are used to mediate EM propagation in order to beat the "diffraction limit [1]" requiring the photon wavelength $\lambda < a$ where a is the optical fiber diameter. If λ is on the order of a micron and a on the order of a nanometer, no propagation is possible. The situation is worse in nano-scale microwave circuits since frequencies are in the GHz (λ about 30 cm) and a on the order of a nanometer.

This work is concentrated on electrical means to control magnonic and spintronic devices exploiting spin-waves and spin-currents for signal processing, logic, memories and telecommunication.

Dealing with such magnetic devices implies the requirement of controlling adequately magnetic fields given the fact that in the microelectronics industry, electric voltage (or field) and not electric current control prevails.

Thus, fabrication of practical devices aims at the goal of replacing magnetic field control by an electrical one (whenever possible) since stray magnetic fields might interfere with device operation besides, technically it is difficult presently to produce large magnetic fields over a nanometer length.

This work is organised as follows. In section 2 electronic control is discussed from the general viewpoint of either replacing magnetic control altogether or combining electricity and magnetism by either coupling or interconverting electrical and magnetic degrees of freedom using specific mechanisms with special types of materials such as composites, metamaterials or single-phase multiferroics. Section 3 is concerned with electronic control of magnonic devices whereas section 4 deals with electronic control of spintronic devices. Conclusions and outlook are presented in section 5.

2. COMBINING ELECTRICITY AND MAGNETISM

1. Coupling electrical and magnetic degrees of freedom

Electric and magnetic degrees of freedom when coupled can be described with the following free energy expansion [2]:

$$-F(\mathbf{E}, \mathbf{H}) = +\frac{1}{2}\epsilon_0\epsilon_{ij}E_iE_j + \frac{1}{2}\mu_0\mu_{ij}H_iH_j + \alpha_{ij}E_iH_j + \frac{1}{2}\beta_{ijk}E_iH_jH_k + \frac{1}{2}\gamma_{ijk}H_iE_jE_k... \quad (1)$$

α_{ij} is first order (in \mathbf{E}, \mathbf{H} components) coupling constant whereas β_{ijk} is first order in \mathbf{E} second order in \mathbf{H} whereas γ_{ijk} is a first order in \mathbf{H} second order in \mathbf{E} components.

ϵ_0 and μ_0 are respectively permittivity and permeability of free space whereas ϵ_{ij} and μ_{ij} are respectively relative permittivity and permeability.

F must satisfy symmetry [2] considerations such as space-inversion symmetry (satisfied in ferromagnets) and time-inversion symmetry (satisfied in ferroelectrics) imposing constraints on the expansion coupling constants. If a multiferroic is both ferroelectric and ferromagnetic, both symmetries are not required [2].

Ferroelectric polarization \mathbf{P} and magnetization \mathbf{M} responses are obtained by differentiating F such as:

$$P_i = \left[\frac{\partial F(\mathbf{E}, \mathbf{H})}{\partial E_i} \right]_{E_i=0} = \alpha_{ij}H_j + \frac{1}{2}\beta_{ijk}H_jH_k + ...$$

$$\mu_0 M_i = \left[\frac{\partial F(\mathbf{E}, \mathbf{H})}{\partial H_i} \right]_{H_i=0} = \alpha_{ji}E_j + \frac{1}{2}\gamma_{ijk}E_jE_k + ... \quad (2)$$

showing how electric degrees of freedom affect magnetic ones and vice versa.

Recall that electric polarization can also be induced in non-uniformly magnetized materials such that $\mathbf{P} \propto [(\mathbf{M} \cdot \nabla)\mathbf{M} - \mathbf{M}(\nabla \cdot \mathbf{M})]$.

Materials containing coupling terms of that nature are magneto-electric (ME) materials whereas a more general class of materials embodying additional coupling with elastic terms are called multiferroic which might be composite or single phase.

In composite materials, coupling between magnetic and electrical degrees of freedom effect or ME coupling is mediated through elastic interaction such as between a magnetostrictive and an electrostrictive (or piezoelectric) substance.

Composite materials made from ferroelectric (or piezoelectric) elements containing lower dimensional magnetic elements such as thin films or multilayers (laminar coupling), wires (fiber or rod coupling) and beads (spherical inclusions) [3] interacting with each other, may be the simplest structures to couple electrical and magnetic degrees of freedom.

In addition to ME composites and multiferroic materials, dilute magnetic semiconductors (DMS [4]) respond to magnetic fields through dispersed magnetic elements that sense the perturbing magnetic field. Magnetic superlattices (also called metamaterials), the magnetic analog of semiconducting superlattices or photonic structures (with spatially variable dielectric constant) contain spatially modulated magnetization, anisotropy or magnetic phase (ferro, antiferro, ferri...) that can alter magnon properties such as dispersion relations (gap and group velocity) allowing spatially dependent adaptive control.

2. Interconverting electrical and magnetic degrees of freedom

A magnetic insulator such as YIG (Ferrimagnetic Yttrium Iron Garnet $\text{Y}_3\text{Fe}_5\text{O}_{12}$ [5, 6]) covered with a noble metal such as Pt can interconvert electrical and magnetic degrees of freedom. A spin current in YIG can be generated (see next section) and detected electrically by using spin and charge current interaction [7]. The signal can travel over a long distance [5, 6] in YIG since it is an insulator devoid of free charges that can act as scattering sources, moreover it has a very low intrinsic magnetic damping coefficient (see Table 2) allowing a spin-wave to travel freely without any loss.

Generally, spin currents belong to three types [8]:

1. SPC (spin-polarized current) made of free (s-type) spin-polarized carriers,
2. SWC (spin-wave current) carried by undulating localized spins (d-type),
3. STT (spin-transfer torque) current stemming from s-d (double) exchange between free and localized carriers [9].

Current densities ought to be very large (in STT they are about 10^6 - 10^7 A/cm²) in order to produce magnetic

switching, this is why the ultimate goal is to rather aim for a small voltage [10] (electric field control [11]) in order to generate a magnetic field or to produce a magnetic effect since it is the conventional control used in traditional microelectronics and because it is spatially localized in contrast with current control that might lead to uncontrolled stray fields.

Magnetic-Electric interconversion between YIG and Pt is based on transfer of spin-angular momentum from (localized) magnetization-precession motion (in YIG) to (free) conduction-electron spins (in Pt) and spin transfer torque (STT). The latter is the reverse process i.e. the transfer of angular momentum from conduction-electron spin (free) back to (localized) magnetization. Many inter-conversion aspects are allowed by the special properties of YIG displayed in Table 2.

Progress in electronic control of magnetic devices summarized in Table 3 shows that many magnetic properties can be tightly controlled with an electric field leading to control of spin-waves and spin-currents as described below.

3. ELECTRONIC CONTROL OF SPIN-WAVES IN THIN FILM DEVICES

Spin waves can be generally divided into three categories [18]:

a- Magnetostatic spin waves (MSW) originating from long-range dipolar interactions between elements whose typical size is the micron. Damon-Eshbach [19] MSW modes are transverse (the wavevector \mathbf{k} is perpendicular to local magnetization \mathbf{M}).

Magnetostatic Surface Spin-Waves (MSSW), the magnetic counterpart of Surface Acoustic Waves (SAW) can also be excited in thin films or stripes made of YIG and their energy is on the order of a few GHz [18].

b- Exchange spin-waves (ESW) originating from short-range Heisenberg exchange interactions between elements whose typical size is the nanometer. Their energy is on the order of a tenth of a GHz (or a μeV) reaching the THz [18] in antiferromagnets.

c- Dipolar-Exchange Spin Waves (DESW) in the case of devices of mixed length type [18], such as Magnetic Quantum Dots (MQD) laid out periodically as planar arrays, with a typical in-plane length (MQD diameter) on the order of a micron and a perpendicular-to-plane length (MQD height) on the order of a nanometer.

In the latter case, spin-waves with both types of contributions occur as predicted for the first time by Herring-Kittel [20] for infinite media and by Clogston *et al.* [21] for finite media such as ellipsoids.

1. Spin-wave generation energetics

Heisenberg model for localized spins in a ferromagnet gives an interaction energy for a pair of neighbouring spins $\mathbf{S}_i, \mathbf{S}_{i+1}$ as $-2J_{ex}\mathbf{S}_i \cdot \mathbf{S}_{i+1}$ where J_{ex} is the exchange integral. The Curie temperature is obtained from $k_B T_c = \frac{2}{3}J_{ex}zS(S+1)$ where z is the coordination number and S the spin value. J_{ex} leads also to spin-wave

energy dispersion: $\hbar\omega_k = 4J_{ex}S(1 - \cos ka)$ where k is the wave vector. Considering a 1D array with lattice parameter a , reversing a single spin costs the spin-flip energy $4J_{ex}S^2$.

For a set of n spins, the total energy is $4nJ_{ex}S^2$ meaning that propagating a spin-flip across a distance na requires such energy. By comparison, spin-wave propagation can be performed with a wavelength chosen to match the

Parameter	Value
Lattice constant	$12.376 \pm 0.004 \text{ \AA}$
Density	5.17 g/cm^3
Band gap	2.85 eV
Saturation induction $4\pi M_S$	1750 G
Cubic anisotropy constant K_1	-610 J/m^3
Anisotropy field $2K_1/M_S$	88 Oe
Cubic anisotropy constant K_2	-26 J/m^3
Curie temperature T_C	563 K
Thermal expansion coefficient	$8.3 \times 10^{-6}/\text{K}$
Relative dielectric constant (at 10 GHz)	14.7
Dielectric loss tangent (at 10 GHz)	0.0002
FMR linewidth ΔH (at 10 GHz)	0.1 Oe
Intrinsic LLG damping constant α	3×10^{-5}
Landé factor g	2.00

TABLE 2: Structural, electric, magnetic, thermal and microwave properties of ferrimagnetic Yttrium Iron Garnet [5, 6] at room temperature in practical units. YIG possesses the narrowest FMR (ferromagnetic resonance) linewidth of all materials with smallest losses and almost zero LLG (Landau-Lifshitz-Gilbert) damping.

same distance $\lambda = na$. The corresponding energy can be evaluated for the wavevector $k = 2\pi/na$ substituted in $4J_{ex}S(1 - \cos ka)$. This gives the energy $2J_{ex}Sk^2a^2$ equal to $8J_{ex}S\pi^2/n^2$ in the limit $ka = 2\pi/n \ll 1$.

As an application, we consider a Ni ribbon as part of a Ni/Permalloy ($\text{Ni}_{81}\text{Fe}_{19}$) bilayer considered as a spin-wave bus (see next subsection) to propagate spin-waves. Despite the fact, Ni is an itinerant magnet where the Heisenberg picture does not strictly apply, we infer that $J_{ex} = 1.45 \times 10^{-21}$ Joules or 9 meV (in comparison, Stoner exchange integral is 1.01 eV [26]) from the above Curie temperature formula with $S = \frac{1}{2}$, $T_C = 629\text{K}$ and coordination number $z = 12$ (from Ni FCC structure).

As an example, the spin-flip propagation energy for 1000 spins is 1.45×10^{-21} Joules whereas the corresponding spin-wave energy (with Ni lattice parameter $a=3.52 \text{ \AA}$) is 5.71×10^{-26} Joules which is about five orders of magnitude smaller.

The spin-wave to spin-flip energy propagation ratio is independent of the value of J_{ex} and strongly decreases with the number n of spins as $\frac{2\pi^2}{Sn^3}$ suggesting that spin-wave propagation is definitely lower in terms of energy cost.

2. Voltage-induced spin wave generation with hybrid cells

Single-phase multiferroics have in general small ME coupling. Instead of using large consumption devices such as inductive antennas or STT currents in order to generate spin-waves, Cherepov *et al.* [11] used hybrid (multiferroic ME) cells consisting of a magnetostrictive Ni layer and a piezoelectric substrate PMN-PT i.e.

$[\text{Pb}(\text{Mg}_{1/3}\text{Nb}_{2/3})\text{O}_3]_{(1-x)} - [\text{PbTiO}_3]_x$.

PMN-PT (lead magnesium niobate-lead titanate) is a ferroelectric relaxor [10] with a large relative dielectric constant ϵ_r . For $0 < x < 0.35$, the electromechanical coupling and piezoelectric coefficients of PMN-PT are very large making it a sensitive material for ME control.

Applying an AC voltage to (PMN-PT) induces an alternating strain in the piezoelectric material. The strain transmitted to the magnetostrictive Ni layer produces local anisotropy variation resulting in easy axis reorientation that pulls on the magnetization. Magnetization oscillations propagate in the form of spin waves in a Ni/Permalloy bilayer lithographically shaped in the form of a stripe that is called a spin-wave bus. While the Ni layer provides the desired magnetostriction, NiFe being a soft magnetic material is favorable to spin-wave propagation because of its low LLG damping constant α .

In order to describe spin-wave generation electronically, we need a process that entails tilting a single spin belonging to an ordered spin array. This entails application of a localized magnetic induction field B_{ex} for a short time.

The value of B_{ex} required to tilt a spin in the ferromagnetic stripe should be on the order of $B_{ex} = B_{dem} \tan \theta$ with θ the tilt angle and B_{dem} the demagnetization field orthogonal to B_{ex} . This originates from the fact the internal field sensed by any spin M is the sum of the external field B_{ex} and the demagnetization field B_{dem} with $B_{dem} = -4\pi NM$. N is the demagnetization coefficient and M the local magnetization.

If we approximate the ferromagnetic stripe by a saturated thin film, the demagnetization coefficient $N = 1$ and $M = M_s$. Thus we infer that the required excitation field is $B_{ex} = 4\pi M_s \tan \theta$.

This field can be generated by an antenna [11] delivering a current pulse or an ME capacitive cell providing voltage pulse whose duration is determined by the operating frequency f_{LO} of the device local oscillator.

At a distance r , Ampère law provides the expression $H_{ex} = \frac{I}{2\pi r}$ relating the required current intensity I to the required magnetic field $H_{ex} = B_{ex}/\mu_0$. Thus the required energy is $\frac{RI^2}{f_{LO}}$ where R is the resistance of the antenna traversed by I .

As an example, we take $\theta = 1^\circ$, $M_s=485 \text{ emu/cm}^3$ (Ni saturation magnetization) and $f_{LO}=5 \text{ GHz}$. At a nominal distance r about 10 times the minimal feature (14 nm), we get the required current $I=7.48 \text{ mA}$.

Taking antenna typical dimensions such as length, height and width ℓ, a, b all around 10 times the minimal feature value and a standard metallic resistivity of $\rho=1 \text{ }\mu\Omega\cdot\text{cm}$, we get antenna resistance $R = \frac{\rho\ell}{ab} \approx 0.07\Omega$ and dissipation energy $\frac{RI^2}{f_{LO}} \approx 8 \times 10^{-16} \text{ Joule}$.

Moving on to the ME capacitive cell made with a material whose ME coefficient $\beta = \frac{\delta H}{\delta E}$ is not small, we may substitute efficiently an electric field to a magnetic

Electrically controlled quantity	Comments	Reference
Exchange interaction	Proposal for electric field modification of local exchange between neighbouring magnets	Gorelik <i>et al.</i> [12] (2003).
Nature of magnetic phase	Ferromagnetic ordering in hexagonal HoMnO ₃ is reversibly controlled by an electric field	Lottermoser <i>et al.</i> [13] (2004).
Coercivity	Electric control of coercivity in CoFeB/MgO/CoFeB magnetic tunnel junction	Wang <i>et al.</i> [14] (2005).
Exchange bias	Electric-field control of exchange bias in multiferroic epitaxial heterostructures	Laukhin <i>et al.</i> [15] (2006).
Sensors, transducers and microwave devices	ME control in composites made with magnetostrictive and piezoelectric elements	Nan <i>et al.</i> [3] (2008).
Magnetic domain wall motion and magnetization direction	Writing/Erase of ferromagnetic domains and electric control of domain wall motion	Lahtinen <i>et al.</i> [16] (2012).
Anisotropy	Electrically induced large magnetization reversal in multiferroic Ba _{0.5} Sr _{1.5} Zn ₂ (Fe _{0.92} Al _{0.08}) ₁₂ O ₂₂	Chai <i>et al.</i> [17] (2014).

TABLE 3: Selected progress milestones in electronic control of magnetic devices.

Electrical control type	Comments	Reference
Spin-Wave logic gates	Current-controlled Mach-Zender type interferometer based on MSSW propagation in YIG thin films	Kostylev <i>et al.</i> [22] (2005).
Spin-Wave phase and wavelength	Current control of phase and wavelength of Damon-Eshbach MSW propagating in Permalloy (Ni ₈₁ Fe ₁₉) ribbons deposited over Cu stripes	Demidov <i>et al.</i> [23] (2009).
Spin-Wave frequency control	Electric-field tuning of ESW frequency at room temperature using multiferroic BiFeO ₃	Rovillain <i>et al.</i> [24] (2010).
Amplification of spin-waves	Electric-field amplification of ESW in YIG/Pt bilayers using Interfacial Spin Scattering	Wang <i>et al.</i> [25] (2011).
Generation of spin-waves	Electric-field-induced ESW generation using multiferroic ME cells	Cherepov <i>et al.</i> [11] (2014).

TABLE 4: Selected progress milestones in electronic control of magnonic devices with several types of spin-waves.

induction field via $E_{ex} = \frac{B_{ex}}{\mu_0\beta}$.

Thus the voltage required for tilting a spin is $V_{ex} = E_{ex}\ell$ where ℓ is the inter-plate distance of a cell whose capacitance $C = \epsilon_r\epsilon_0 ab/\ell$ with energy $\frac{1}{2}CV^2$.

A material such as Fe₃O₄/PMN-PT has an ME coefficient $\beta = 67$ Oe.cm/kV (see Liu *et al.* [10]) and a relative dielectric constant around several 1000.

Taking all dimensions such as length, height and width ℓ, a, b about 10 times the minimal feature value, we get a capacitance $C = \frac{\epsilon_r\epsilon_0 ab}{\ell} = 1.23 \times 10^{-15}$ F, a voltage of 22.2 mV and a tilting energy of $\frac{1}{2}CV^2 = 3 \times 10^{-15}$ Joule which is three orders of magnitude below the antenna case.

The capacitive over resistive (antenna) energy ratio

$\eta = \frac{1}{2}CV^2 / \frac{RI^2}{f_{LO}}$ can be expressed in a scaling form as $\eta = \frac{\epsilon_0\epsilon_r\ell^2 f_{LO}}{8\pi^2\rho\beta^2}$ where ℓ replaces all lengths in the device implying that as minimal feature continues to decrease $\eta \sim \ell^2$ will decrease.

Moreover $\eta \sim \frac{\epsilon_r}{\beta^2}$ implying that we need multiferroic materials with a smaller ϵ_r and a larger ME coefficient β in order to keep η decreasing, in contrast to materials such as PMN-PT with both (ϵ_r, β) large.

Once the spin is tilted, its time variation follows space-dependent LLG equation:

$$\frac{\partial \mathbf{M}(\mathbf{r}, t)}{\partial t} = -\gamma \mathbf{M}(\mathbf{r}, t) \times \mathbf{H} - \frac{\alpha \gamma}{|\mathbf{M}|} \mathbf{M}(\mathbf{r}, t) \times [\mathbf{M}(\mathbf{r}, t) \times \mathbf{H}] \quad (3)$$

where γ is the gyromagnetic ratio, \mathbf{M} the magnetization vector, \mathbf{H} the effective field obtained from total energy and α the intrinsic damping parameter (see Table 2). LLG equation describes a propagating Bloch equation for a moment precessing around magnetic field \mathbf{H} direction and damped by the α term that forces the moment to precess closer to the magnetic field direction thus reducing the initial tilt angle θ . Choosing materials such as Ni, Ni/NiFe bilayers as well as YIG that possess small α , allows long-distance signal propagation since θ diminishes very weakly in the course of time.

4. ELECTRONIC CONTROL OF SPINTRONIC DEVICES

1. Issues in electric-field controlled spintronic devices

Substituting magnetic field control by an electrical one is possible in semiconductors via spin-orbit interaction since it allows generation and manipulation of carrier spins by an electric field [27].

Spin-orbit interaction has also been shown to allow electric control of spin-waves in single-crystal YIG waveguides which paves the way to develop electrically tunable magnonic devices [28, 29].

Another alternative is a tunable spin current that allows to generate a magnetic field or produce a magnetic effect (such as reversal or alteration of magnetization) since a spin current targets interconversion between charge and spin degrees of freedom [8, 30].

In analogy with ordinary electronics, spintronics is based on several operations such as spin injection, filtering, accumulation, detection and pumping [27].

The notion of spin coherence underlies all these operations, that is preservation of a given spin state over long distances despite the presence of impurities, dislocations, noise, stray magnetic fields, Earth magnetic field etc...

Spin injection might be done optically in complete analogy with Haynes-Shockley experiment. It may also be done with carbon nanotubes since they do not alter the spin state over large distances (see Dietl *et al.* [30]).

Spin filtering is essentially the separation of spin-polarised carriers which is required for avoiding spin-flips that alter carrier spin states akin to geminate recombination between photo-generated electron-hole pairs. Thin ferromagnetic layers as in spin valves (see Dietl

et al. [30]) and chiral materials such as monolayers of double-stranded DNA molecules can be used [31].

Spin accumulation is concerned with increase of concentration of spin polarized carriers without destroying their coherence or inducing spin-flips among them whereas spin detection relates to non-destructive determination of spin value.

Spin pumping [32] occurs in Ferromagnetic-Normal bilayers, when the precessing magnetization in the Ferromagnet (F) injects a spin-current into a normal metal (N) through the F-N interface (as in the YIG/Pt case described previously).

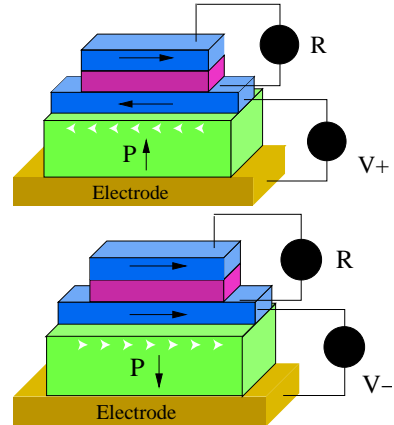


FIG. 1: (Color on-line) MeRAM cell showing the electric field control and the different materials composing the memory cell. A spin-valve made from two blue layers (ferromagnets) separated by a metallic spacer (in magenta) has its resistance R monitored. The upper blue layer made from a hard magnetic material is free and the lower blue layer is made from a soft magnetic material in close contact with a (green layer) material made from a ferroelectric antiferromagnet, a single-phase multiferroic. Top figure shows positive voltage V applied to electrode (gold yellow) with blue layer magnetizations (black arrows) antiparallel resulting in a high resistance R . Bottom figure shows negative voltage V applied while blue layers have parallel magnetizations yielding a very low resistance R . Magnetization (black arrow) in each lower blue layer follows green material magnetization represented by small white arrows. In a multiferroic, polarization \mathbf{P} and magnetization are coupled [33]. Thus when \mathbf{P} is up (V positive), magnetization (represented by small white arrows) is oriented to the left and when \mathbf{P} is down (V negative), magnetization is oriented to the right. Adapted from Bibes *et al.* [34]

Many of the spin manipulation processes described above intervene in the progress milestones for electric-field control of spintronic devices displayed in Table 5.

2. Electric-field controlled magneto-electric RAM devices

Magnetic Random-Access Memories (MRAM) abolish the distinction between volatile storage (used during

processing) and permanent massive storage. A RAM

Electrical control type	Comments	Reference
Driving of microwave oscillation	GHz oscillator excited by STT current	Kiselev <i>et al.</i> [35] (2003).
Magnetic Random-Access Memories (MRAM)	Electric control of CoFeB/MgO/CoFeB tunnel magnetoresistance switching	Wang <i>et al.</i> [14] (2005).
Spin transport in nanotubes	Electric-field control of magnetoresistance in carbon nanotubes connected by ferromagnetic leads	Sahoo <i>et al.</i> [36] (2005).
Spin transport in Silicon	Ballistic spin-dependent hot-electron filtering through ferromagnetic thin films	Appelbaum <i>et al.</i> [37] (2007).
Memory Read-Write operations	Information processing in MRAM cell made with a DMS: (Ga,Mn)As	Mark <i>et al.</i> [38] (2011).
Spintronic logic gates	Voltage-controlled spin selection and tuning in graphene nanoribbons for logic	Zhang [39] (2014).

TABLE 5: Selected progress milestones in electronic control of spintronic devices

is used by a CPU or a DSP (Digital Signal Processor) during processing, for loading an operating system (OS) or enabling application programs (AP). The implication that the OS and the AP are permanently loaded in MRAM brings a paradigm shift in computing that has far reaching consequences in terms of computing speed and efficiency. The initial attempts to design MRAM cells were based on domain wall motion control with a strong electric current (racetrack-type memories [30]). MeRAM memory is a new type of voltage controlled RAM based on ME multiferroic interacting with a ferromagnet. The multiferroic is a ferroelectric antiferromagnet whose electric polarization induces an internal magnetization (see fig. 1) that controls the neighbouring ferromagnet magnetization at the interface. An example ferroelectric antiferromagnet is BiFeO₃ (BFO) that displays both ferroelectricity and antiferromagnetic order at room temperature [40].

BFO has a rhombohedral perovskite crystallographic structure. It is a high-temperature ferroelectric (with Curie temperature $T_c \approx 1100$ K) possessing a large ferroelectric dipole moment $\approx 100 \mu\text{C}/\text{cm}^2$. At room temperature, bulk crystalline BFO is antiferromagnetic [40] with Néel temperature T_N of 640 K. Voltage control of BFO magnetic state has been shown both in bulk and in thin film case making it an excellent candidate for ME applications.

The ferroelectric polarization and the antiferromagnetic vector in BFO are coupled [33] in a way such that by reversing the polarization, the antiferromagnetic spins rotate. Nevertheless the antiferromagnetic structure of BFO is complicated [40] making the work of Chu *et al.* [41] more appealing.

The latter [41] have shown that micrometre-size ferro-

magnetic CoFe dots deposited on a BFO film are consistently coupled, in a reversible manner, with the BFO antiferromagnetic spins. This implies that when an in-plane electric field is applied, CoFe dot magnetization rotates by 90° and when voltage polarity is reversed the original CoFe magnetic state is retrieved.

5. CONCLUSIONS AND OUTLOOK

Electric control of magnonic and spintronic devices is steadily progressing [10], offering lower energy consumption devices and paving the way to potentially solve the nagging interconnection delay problem.

Simultaneously, femtosecond optical control is also progressing in antiferromagnets that represent the largest class of spin ordered materials in Nature with spin-wave excitations occurring typically at frequencies as high as a THz. Eventually, this will lead to extremely fast control [42] of magnetic devices to reach the THz regime unlocking the frequency stalling problem around a few GHz in present CMOS devices.

Kampfrath *et al.* [42] used optical femtosecond pulses to control spin-waves in antiferromagnetic NiO and more recently Shuvaev *et al.* [43] demonstrated electrical control of a dynamic ME effect in DyMnO₃, a single-phase multiferroic material. ME coupling with spin-waves leads to rotation of polarization plane of light propagating across a sample and a static voltage allows to control light amplitude and polarization plane rotation.

The THz barrier is the last one to overcome among four making the pillars of Digital Technology that is continuously thriving toward THz operation speed, Teraflop processing, Terabyte storage and finally Terabit/sec communication.

[1] D. K. Gramotnev and S. I. Bozhevolnyi, "Plasmonics beyond the diffraction limit", *Nature Photonics*, **4**, 83

(2010).

[2] W. Eerenstein, N. D. Mathur and J.F. Scott, "Multifer-

- roic and magneto-electric materials", *Nature* **442**, 759 (2006).
- [3] C-W Nan, M. I. Bichurin, S.X. Dong, D. Viehland and G. Srinivasan, *J. Appl. Phys. Applied Physics Reviews*, **103**, 031101 (2008).
 - [4] C. Liu, F. Yun, and H. Morkoç: "Ferromagnetism of ZnO and GaN: A Review", *J. Mater. Sci. : Mater. Electron.* **16**, 555 (2005).
 - [5] Ü. Özgür, Y. Alivov and H. Morkoç "Microwave Ferrites, Part 1: Fundamentals and self biasing", *J. Mater. Sci. : Mater. Electron.* **20**, 789 (2009).
 - [6] Ü. Özgür, Y. Alivov and H. Morkoç "Microwave Ferrites, Part 2: : Passive components and electrical tuning", *J. Mater. Sci. : Mater. Electron.* **20**, 911 (2009).
 - [7] Y. Kajiwara, K. Harii, S. Takahashi, J. Ohe, K. Uchida, M. Mizuguchi, H. Umezawa, H. Kawai, K. Ando, K. Takanashi, S. Maekawa, E. Saitoh, *Nature* **464**, 262 (2010).
 - [8] M.Z. Wu and A. Hoffmann, *Solid State Physics Volume 64, Recent Advances in Magnetic Insulators - From Spintronics to Microwave Applications*, Academic Press and Elsevier, New-York (2013).
 - [9] J. C. Slonczewski, *J. Magn. Magn. Mat.* **195**, L261 (1999).
 - [10] M. Liu, N. X. Sun, "Voltage control of magnetism in multiferroic heterostructures", *Phil. Trans. R. Soc. A* **372**, 20120439 (2014).
 - [11] S. Cherepov, P. K. Amiri, J. G. Alzate, K. Wong, M. Lewis, P. Upadhyaya, J. Nath, M. Bao, A. Bur, T. Wu, G. P. Carman, A. Khitun and K. L. Wang "Electric-field-induced spin wave generation using multiferroic magneto-electric cells" *Appl. Phys. Lett.* **104**, 082403 (2014).
 - [12] L. Y. Gorelik, R. I. Shekhter, V. M. Vinokur, D. E. Feldman, V. I. Kozub and M. Jonson, *Phys. Rev. Lett.* **91**, 088301 (2003).
 - [13] T. Lottermoser, T. Lonkai, U. Amann, D. Hohlwein, J. Ihlinger and M. Fiebig, "Magnetic phase control by an electric field", *Nature* **430**, 541 (2004).
 - [14] W-G Wang, M. G. Li, S. Hageman and C. L. Chien, "Electric-field-assisted switching in magnetic tunnel junctions", *Nature Mater.* **11**, 64 (2012).
 - [15] V. Laukhin, V. Skumryev, X. Marti, D. Hrabovsky, F. Sanchez, M.V. Garcia-Cuenca, C. Ferrater, M. Varela, U. Lüders, J.F. Bobo and J. Fontcuberta, *Phys. Rev. Lett.* **97**, 227201 (2006).
 - [16] T. H. E. Lahtinen, K. J. A. Franke and S. van Dijken, "Electric-field control of magnetic domain wall motion and local magnetization reversal", *Sci. Rep.* **2** 258; doi:10.1038/srep00258 (2012).
 - [17] Y. S. Chai, S. Kwon, S. H. Chun, I. Kim, B-G Jeon, K. H. Kim and S. Lee, "Electrical control of large magnetization reversal in a helimagnet", *Nat. Commun.* **5**:4208 doi: 10.1038/ncomms5208 (2014). See also S. E. Barnes, J. Ieda and S. Maekawa, "Rashba Spin-Orbit Anisotropy and the Electric Field Control of Magnetism", *Sci. Rep.* **4**, 4105; doi:10.1038/srep04105 (2014) who did a theoretical analysis for electrical anisotropy control in thin magnetic films.
 - [18] B. Lenk, H. Ulrichs, F. Garbs, M. Münzenberg, "The building blocks of magnonics" *Physics Reports* **507** 107 (2011).
 - [19] R.W. Damon, J.R. Eshbach, *J. Phys. Chem. Solids* **19** 308 (1961).
 - [20] C. Herring and C. Kittel, *Phys. Rev.* **81**, 869 (1951).
 - [21] A. M. Clogston, H. Suhl, L. R. Walker and P.W. Anderson, *J. Phys. Chem. Solids* **1**, 129 (1956).
 - [22] M. P. Kostylev, A. A. Serga, T. Schneider, B. Leven, and B. Hillebrands, *Appl. Phys. Lett.* **87**, 153501 (2005).
 - [23] V. E. Demidov, S. Urazhdin and S. O. Demokritov, *Appl. Phys. Lett.* **95**, 262509 (2009).
 - [24] P. Rovillain, R. de Sousa, Y. Gallais, A. Sacuto, M. A. Méasson, D. Colson, A. Forget, M. Bibes, A. Barthélémy and M. Cazayous, "Electric-field control of spin waves at room temperature in multiferroic BiFeO₃", *Nature Mater.*, **9**, 975 (2010).
 - [25] Z. Wang, Y. Sun, M; Wu, V. Tiberkevich and A. Slavin, *Phys. Rev. Lett.* **107**, 146602 (2011).
 - [26] J.M.D. Coey, "Magnetism and Magnetic Materials", Cambridge University Press, New-York (2009).
 - [27] D. Awschalom and N. Samarth, "Spintronics without magnetism" *APS Physics* **2**, 50 (2009).
 - [28] T. Liu and G. Vignale, *Phys. Rev. Lett.* **106**, 247203 (2011).
 - [29] X. Zhang, T. Liu, M. E. Flatté and H. X. Tang, *Phys. Rev. Lett.* **113**, 037202 (2014).
 - [30] T. Dietl, D. D. Awschalom, M. Kaminska and H. Ohno, "Spintronics" in "Semiconductors and Semimetals: A treatise", Volume 82, edited by E. R. Weber, Academic Press and Elsevier (2008).
 - [31] B.Gohler, V. Hamelbeck, T.Z. Markus, M. Kettner, G.F. Hanne, Z. Vager, R. Naa-man, H. Zacharias, *Science* **331** 894 (2011).
 - [32] Y Tserkovnyak, A. Brataas and G. E. W. Bauer, *Phys. Rev. Lett.* **88**, 117601 (2002).
 - [33] T. Zhao, A. Scholl, F. Zavaliche, K. Lee, M. Barry, A. Doran, M. P. Cruz, Y. H. Chu, C. Ederer, N. A. Spaldin, R. R. Das, D. M. Kim, S. H. Baek, C. B. Eom and R. Ramesh "Electrical control of antiferromagnetic domains in multiferroic BiFeO₃ films at room temperature", *Nature Mater.*, **5**, 823 (2006).
 - [34] M. Bibes and A. Barthélémy, "Towards a magneto-electric memory", *Nature Mater.*, **7**, 425 (2008).
 - [35] S. I. Kiselev, J. C. Sankey, I. N. Krivorotov, N. C. Emley, R. J. Schoelkopf, R. A. Buhrman and D. C. Ralph, *Nature* **425**, 380 (2003).
 - [36] S. Sahoo, T. Kontos, J. Furer, C. Hoffmann, M. Gräber, A. Cottet and C. Schönenberger, "Electric field control of spin transport" *Nature Physics* **1**, 99 (2005).
 - [37] I. Appelbaum, B. Huang and D. J. Monsma, "Electronic measurement and control of spin transport in silicon", *Nature Mater.*, **447**, 295 (2007).
 - [38] S. Mark, P. Durrenfeld, K. Pappert, L. Ebel, K. Brunner, C. Gould and L. W. Molenkamp *Phys. Rev. Lett.* **106**, 057204 (2011).
 - [39] W. X. Zhang, "Voltage-driven spintronic logic gates in graphene nanoribbons", *Sci. Rep.* **4**, 6320, doi:10.1038/srep06320 (2014).
 - [40] D. Talbayev, S. A. Trugman, S. Lee, H T Yi, S.-W. Cheong and A. J. Taylor, *Phys. Rev.* **B 83**, 094403 (2011).
 - [41] Y.H. Chu, L.W. Martin, M.B. Holcomb, M. Gajek, S-J Han, Q. He, N. Balke, C.H Yang, D. Lee, W. Hu, Q. Zhan, P-L Yang, A. Fraile-Rodriguez, R. Scholl, S.X. Wang and R. Ramesh "Electric-field control of local ferromagnetism using a magneto-electric multiferroic", *Nature Mater.*, **7**, 478 (2008).
 - [42] T. Kampfrath, A. Sell, G. Klatt, A. Pashkin, S. Mahrlein,

- T. Dekorsy, M. Wolf, M. Fiebig, A. Leitenstorfer and R. Huber, "Coherent Terahertz control of antiferromagnetic spin waves", *Nature Photonics*, **5**, 31 (2011).
- [43] A. Shuvaev, V. Dziom, A. Pimenov, M. Schiebl, A. A. Mukhin, A. C. Komarek, T. Finger, M. Braden, and A. Pimenov, *Phys. Rev. Lett.* **111**, 227201 (2013).